GIGANTEA is a nuclear protein involved in phytochrome signaling in *Arabidopsis*

Enamul Huq, James M. Tepperman, and Peter H. Quail*

Department of Plant and Microbial Biology, University of California, Berkeley, CA 94720; and U.S. Department of Agriculture/Agricultural Research Service, Plant Gene Expression Center, 800 Buchanan Street, Albany, CA 94710

Communicated by Winslow R. Briggs, Carnegie Institution of Washington, Stanford, CA, June 20, 2000 (received for review March 23, 2000)

In a genetic screen of available T-DNA-mutagenized *Arabidopsis* populations for loci potentially involved in phytochrome (phy) signaling, we identified a mutant that displayed reduced seedling deetiolation under continuous red light, but little if any change in responsiveness to continuous far-red light. This behavior suggests disruption of phyB, but not phyA signaling. We have cloned the mutant locus by using the T-DNA insertion and found that the disrupted gene is identical to the recently described *GIGANTEA* (*GI*) gene identified as being involved in control of flowering time. The encoded GI polypeptide has no sequence similarity to any known proteins in the database. However, by using β−glucuronidase-GI and green fluorescent protein-GI fusion constructs, we have shown that GI is constitutively targeted to the nucleus in transient transfection assays. Optical sectioning by using the green fluorescent protein-GI fusion protein showed green fluorescence throughout the nucleoplasm. Thus, contrary to previous computer-based predictions that GI would be an integral plasmamembrane-localized polypeptide, the data here indicate that it is a nucleoplasmically localized protein. This result is consistent with the proposed role in phyB signaling, given recent evidence that early phy signaling events are nuclear localized.

One of the major environmental factors controlling plant growth and development is light. Plants have evolved at least three photoreceptor systems to track the wavelength, intensity, and duration of ambient light conditions. These include red/far-red absorbing phytochromes (phys), UV-A/blue light receptors, and as yet unidentified UV-B receptors (1). The phys, which consist of five members, phyA to phyE, in *Arabidopsis* (2, 3), are the most extensively characterized. The unique capacity of these soluble chromoproteins to interconvert between their red-light (R)-absorbing form, Pr, and their far-red light (FR)-absorbing form, Pfr, endows the phytochromes with the properties of a molecular switch that regulates a diverse set of responses from seed germination to photoperiodic flowering in higher plants (1, 4).

Analyses of mutations in individual phytochromes, as well as putative signaling intermediates, and molecular identification of various factors that interact with phytochromes have provided an outline of the signaling pathway. These studies suggest that phy signaling might include a direct pathway transferring light signals from the photoreceptors to putative transcription factors for controlling gene expression (5–7). The availability of mutants specifically defective either in R responsiveness [e.g., *pef2* and *pef3* (8), *red1* (9), *poc1* (10), *srl1* (11)], or in FR responsiveness [e.g., *fhy1* and *fhy3* (12), *far1* (13), *fin2* (14), *spa1* (15)], or in both R and FR responsiveness [e.g., *pef1* (8), *psi2* (16)] suggests that at least phyA and phyB have distinct, genetically separable, early signal transduction pathways that converge downstream (6, 17). Interestingly, many of the putative signaling factors, such as SPA1 (18), FAR1 (13), and PIF3 (19), have been shown to be constitutively nuclear localized. Moreover, it has also been shown that phyA and phyB migrate to the nucleus in response to light (20–22), suggesting that early phy signaling includes events focused in the nucleus.

Although a number of mutants are available that are defective in phy signaling, none of these pathways seem to be saturated. In an effort to identify additional phyB-signaling mutants, we have screened available activation-tagged pools of *Arabidopsis* seeds. From this screen, we isolated a mutant, initially designated G6, which displayed long hypocotyls selectively under R-light. This mutant was also found to flower late under greenhouse conditions. After the molecular cloning of the G6 locus, two reports appeared describing the cloning of the *GIGANTEA* (*GI*) locus, identified by mutation as being involved in controlling flowering time (23, 24). Sequence comparison established that the G6 locus is identical to *GI*. Here, we suggest that GI has a more general role in phyB signaling, potentially explaining its involvement in floral induction, and we begin to explore the cellular basis of its putative signaling role by investigating its subcellular localization.

Materials and Methods

Growth of Seedlings and Genetic Screening. Seeds were sterilized and plated on growth medium without sucrose as described (15). The plates were kept in the dark at 4°C for stratification. After an initial 3 h of continuous white light (Wc) treatment, plates were returned to the dark for 21 h at 21°C and then transferred to various light conditions. The light sources used are as described (25), and the fluence rates were monitored by using a spectroradiometer (model LI-1800; Li-Cor, Lincoln, NE). Hypocotyl lengths were measured by using a Pixera digital camera (Pixera, Cupertino, CA) and National Institutes of Health IMAGE software (Bethesda, MD).

The pools of activation-tagged seeds were obtained from the *Arabidopsis* Biological Resources Center (stock no. CS21995). These seeds were generated in a Columbia (Col) ecotype background (26). Initially, the screening was performed under continuous R (Rc) (13.84 $\mu molm^{-2}s^{-1}$). The selected seedlings were selfed and tested under both Rc and continuous FR (FRc) for hypocotyl phenotype.

For determination of flowering time, seedlings used for hypocotyl experiments were transplanted to soil and grown in growth chambers under short day (SD) (9 h Wc of 128 $\mu molm^{-2}{\cdot}s^{-1}$ and 15 h dark) or long day (LD) (18 h Wc of 62 $\mu molm^{-2}{\cdot}s^{-1}$ and 6 h dark) conditions at 21°C. The number of rosette leaves and days from plating were counted when the plants bolted.

Cloning of the Mutant Locus and Corresponding cDNA. The flanking genomic sequence at the T-DNA insertion site was amplified by

Abbreviations: Rc, continuous red light; FRc, continuous far-red light; Wc, continuous white light; phy, phytochrome; Col, Columbia; GI, GIGANTEA; SD, short day; LD, long day; GUS, β-glucuronidase; NLS, nuclear localization signal.

*To whom reprint requests should be addressed. E-mail: quail@nature.berkeley.edu.

The publication costs of this article were defrayed in part by page charge payment. This article must therefore be hereby marked "*advertisement*" in accordance with 18 U.S.C. §1734 solely to indicate this fact.

Article published online before print: *Proc. Natl. Acad. Sci. USA*, 10.1073/pnas.170283997. Article and publication date are at www.pnas.org/cgi/doi/10.1073/pnas.170283997

the PCR-based genome Walker kit (CLONTECH). A 1.6-kb genomic fragment was amplified by using a T-DNA specific primer from a *Pvu*II-digested genome Walker library. Sequencing of this fragment was performed by using an Amersham Pharmacia sequencing kit and a 373 DNA sequencer (Perkin–Elmer). A reverse primer covering the ATG start codon was used to isolate the full-length cDNA from a λZapII cDNA library (27) (ABRC stock no. CD4–16) following the protocol described in Gene Trapper cDNA Positive Selection System (Life Technologies, Grand Island, NY).

RNA Extraction and Northern Blotting. RNA extractions from 3-day-old seedlings were performed by using a Qiagen (Chatsworth, CA) RNeasy Miniprep kit. Five micrograms of total RNA was separated on a Mops-formaldehyde (6.7%) agarose (1.0%) gel and transferred to MSI Nylon membrane. The membranes were hybridized according to Church and Gilbert (28) and washed finally with 0.2× saline sodium citrate containing 0.1% SDS at 65°C. The full-length ORFs of neighboring genes (see Fig. 2*A*) and the 5′ fragment of the *gi-100* allele were amplified by PCR and used as probes after labeling with the Multiprime DNA labeling System (Amersham Pharmacia). The transcript levels were determined by PhosphorImager (Storm 860; Molecular Dynamics) quantification and normalized to 18S rRNA levels.

Construction of Vector for Transgenic Complementation. An 8.6-kb fragment from nucleotide 10591 to 19212 of BAC T22J18, which includes the coding region, 255 bp of the 3′-untranslated region, and 3,216 bp of the 5′ flanking DNA, including the presumptive promoter region of the *gi* locus, was amplified by using PFU Turbo polymerase (Stratagene) from Col genomic DNA. *Kpn*I and *Bam*HI restriction enzyme sites were included in the primer, the resulting fragment was cloned into the pPZP121 vector (29), and the coding region of *GI* was sequenced. The resulting construct was introduced into GV3001 *Agrobacterium* and used for transformation of the *gi-100* mutant by the floral dip method (30). Transgenic seeds were plated on GM-Suc plates containing 100 μg/ml of gentamycin. The resistant seedlings were transplanted to soil and grown in the greenhouse.

Subcellular Localization. The full-length coding region or defined fragments thereof of the *GI* transcript were amplified from the cDNA clone by PCR by using PFU Turbo polymerase (Stratagene). Restriction enzyme sites were introduced in both forward and reverse primers and were used to clone in either pRTL2- for β−glucuronidase (GUS) fusions (31) or pAVA120 vector (32) for green fluorescent protein (GFP) fusions as *Bgl*II–*Xba*I fragments. The resulting constructs were sequenced and used for transient transfection assays as described (19). For confocal microscopy of the GFP-GI protein, onion epidermal cells were stained with propidium iodide (PI) (0.1 μg/ml) and scanned by using a Zeiss 510 confocal laser scanning microscope with a Krypton/Argon laser at 1024 × 1024 pixel resolution with a 25× oil objective. The wavelengths used were: 488 nm excitation for GFP, 568 nm excitation for PI, 505–550 nm band pass filter for GFP emission, and 585 nm and above band pass filter for PI emission. All of the images were taken by using Zeiss LSM software and assembled by using ADOBE PHOTOSHOP software (Adobe Systems, Mountain View, CA).

Results

Mutant Isolation and Cloning of the Locus. The mutant, designated G6, was isolated as exhibiting a long hypocotyl under Rc (14 $\mu molm^{-2}{\cdot}s^{-1}$) by screening activation-tagged seed pools (26). The *bar* gene present in the T-DNA was used to assess the number of insertion sites in the mutant. The homozygous mutant was backcrossed to wild-type Col and the resulting F_2 progeny were analyzed on GM-Suc containing basta (5 mg/liter). The basta resistant phenotype segregated with a 3:1 ratio, indicating that the insertion is at a single locus in the mutant. The hypocotyl length of F_1 seedlings was intermediate between that of the wild-type and homozygous mutant, indicating that the G6 mutant might be semidominant.

We isolated the sequence flanking the T-DNA insertion by using a PCR-based Genome Walker kit (CLONTECH). A 1.6-kb fragment was isolated by using a T-DNA specific primer located near the left border. BLAST searches using the sequence of this fragment showed identity to a region on BAC T22J18 at the top of chromosome 1 annotated as ORF T22J18.6 (GenBank accession no. AC003879).

We also cloned and sequenced a full-length cDNA (data not shown). The 4-kb cDNA has an ORF of 3422 bp encoding a predicted 1,173-aa residue protein of 127 kDa. Subsequently, we determined that the nucleotide and predicted amino acid sequence are identical with the GI sequence recently reported by Fowler *et al.* (23) and Park *et al.* (24). Therefore, we have renamed our G6 mutant *gi-100*, to reflect its being a new allele of the *gi* mutant family.

***gi-100* Is Primarily Defective in phyB Signaling.** *gi-100* was isolated as a long hypocotyl mutant under Rc using a single fluence rate. Fig. 1*A* presents a fluence-rate response curve showing that *gi-100* has reduced sensitivity to all of the fluence rates of Rc used. In contrast, little or no differential responsiveness to increasing FRc between wild-type and *gi-100* seedlings was observed for the fluence rates investigated (Fig. 1*B*). This contrast in sensitivity of the *gi-100* mutant to Rc and FRc relative to wild type is most apparent when the data are normalized to the respective dark value for each line (Fig. 1 *A* and *B*, *Insets*). These data indicate that the *gi-100* phenotype is light-dependent and Rc-selective (Fig. 1 *A–C*). Because phyB is quantitatively the principal phytochrome regulating seedling deetiolation responses to Rc, and phyA is the exclusive mediator of FRc signals (4), the present data suggest that the *gi-100* mutation causes a selective reduction in phyB signaling with little or no effect on phyA signaling.

We have also tested the hypocotyl phenotype of two other *gi* mutant alleles, *gi-1* and *gi-2*. Both showed slightly reduced Rc-sensitivity to a level that is intermediate between *gi-100* and wild type (Fig. 1 *A* and *C*). In contrast, *gi-1* and *gi-2* did not show any significant hypocotyl phenotype under FRc (Fig. 1*B*).

We examined the levels of both phyA and phyB by immunoblot and detected no significant reduction in the levels of these phytochromes in *gi-100* compared with the wild type (data not shown). Thus, the hyposensitive phenotype of *gi-100* is not because of altered expression of these photoreceptors. Therefore, we suggest that *gi-100* is a signaling mutant defective in a factor that is required to facilitate signaling selectively, if not specifically, from phyB to downstream components.

Expression of *GI* and Neighboring Genes. Because *gi-100* was isolated from a transgenic line generated with an activation-tagged vector, we compared the expression patterns of the *GI* gene and predicted ORFs on either side of the *gi-100* locus between wild type and mutant. The *gi-100* locus (g6; Fig. 2*A*) expressed a ≈2-kb stable transcript compared with the 4-kb transcript present in the wild type (Fig. 2*B*). The 3′ end of the *GI* transcript is not expressed in the *gi-100* mutant (data not shown). In addition, the levels of the *gi-100* transcript, as well as that of g4 and g5 transcripts, are somewhat higher in the *gi-100* mutant than the wild type, whereas the level of g8 is slightly reduced (Fig. 2 *A–C*). g7 did not give any signal in either wild type or mutant. Thus, although insertional disruption of the *GI* locus appears to be the most likely cause of the mutant phenotype, the present data do not rule out contributions from the slightly altered expression of the neighboring genes.

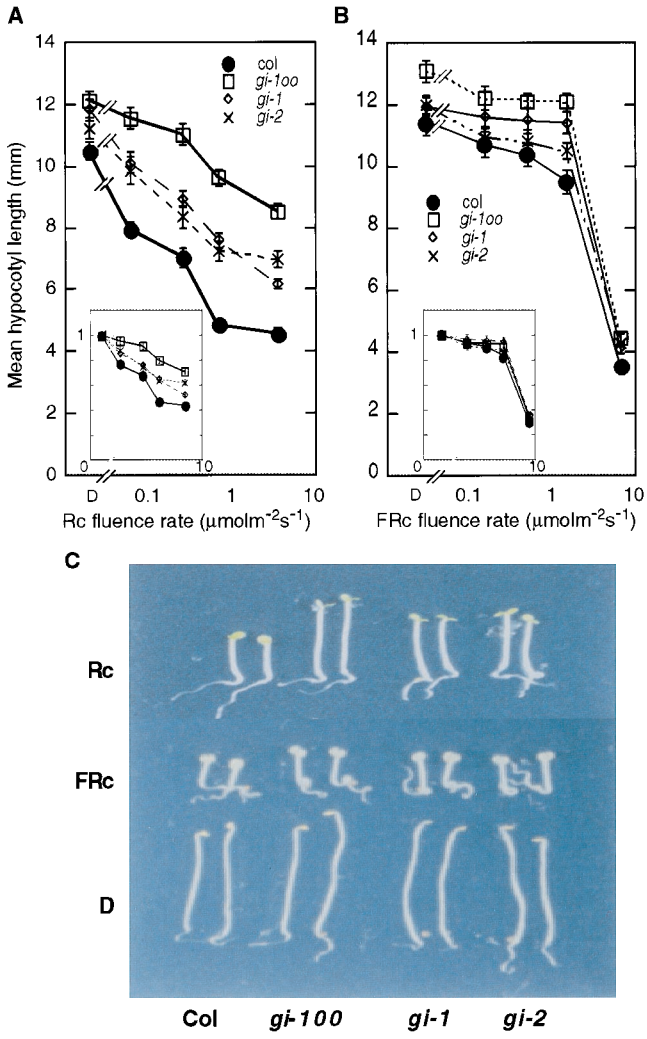

Fig. 1. *gi* mutant seedlings are selectively hyposensitive to red light. Hypocotyl lengths of wild-type (Col) and *gi* mutants with different alleles (*gi-1*, *gi-2*, *gi-100*) grown for 3 days in the dark (D) or a range of Rc (*A*) or FRc (*B*) fluence rates. Hypocotyl length expressed as percentage of dark value is shown in the insets. Data are expressed as mean ± SEM. (*C*) Seedlings grown either in dark (D), or in Rc (3.84 μmolm^{-2}s^{-1}) or FRc (6.8 μmolm^{-2}s^{-1}) for 3 days.

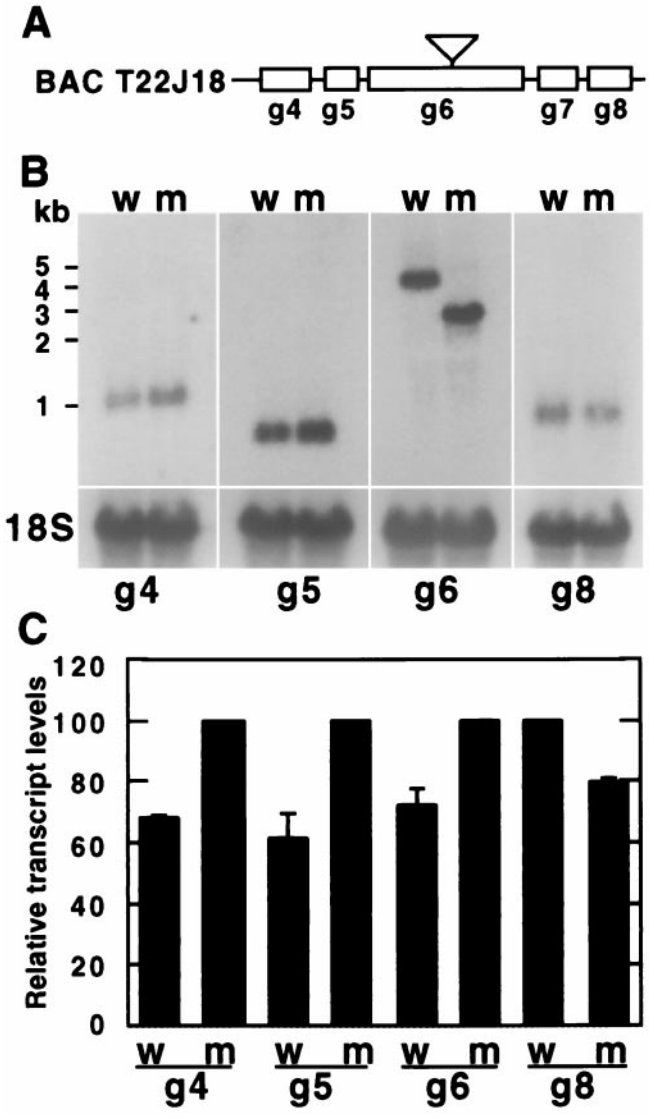

Fig. 2. Expression of *GI* and neighboring genes is altered in *gi-100* mutant seedlings. (*A*) Diagrammatic representation of the insertionally tagged *gi-100* gene (g6) and neighboring genes (g4, g5, g7, g8) within the sequenced BAC T22J18. The inverted triangle shows the location of the T-DNA insert in the *gi-100* mutant. g4 = T22J18.4; g5 = T22J18.5; g6 = T22J18.6 (*GI*); g7 = T22J18.7; g8 = T22J18.8. (*B*) Northern blots of *GI* and neighboring-gene transcripts in both wild-type and *gi-100* mutant seedlings. An 18S rDNA probe was used to reprobe each blot to show the amount of RNA loaded in each lane. Approximate marker sizes are shown on the left. (*C*) Quantification of transcript levels using a PhosphorImager. Signals for each transcript were normalized with the 18S rDNA signal and expressed as a percentage of the highest value obtained for each gene. Data are expressed as mean ± SEM ($n \geq 2$).

Complementation of *gi-100* by the *GI* Locus. Because of this uncertainty, we transformed the *gi-100* mutant with the wild-type genomic locus containing the natural promoter and coding region of the *GI* gene, and selected 13 independent transgenic lines that were gentamycin resistant. From these, we selected two homozygous lines (C23 and C33) with single copy insertions (based on segregation on gentamycin) for further analysis of hypocotyl lengths. As shown in Fig. 3*A*, the hypocotyl lengths of these two lines were very similar to the wild type under all Rc fluence rates used, whereas *gi-100* showed longer hypocotyls under the same conditions as expected. These data indicate that the insertional disruption at the *gi-100* locus is indeed the major, if not exclusive, cause of the hyposensitive response of the hypocotyls to Rc.

We initially observed that homozygous *gi-100* flowered late under Wc in greenhouse conditions. We also measured flowering time of this mutant under both SD and LD conditions. Under SD, *gi-100* flowered 2–3 days later than the wild type with seven to eight more rosette leaves (Fig. 3*C*). However, the time to flowering was greatly increased in *gi-100* relative to wild type under LD. *gi-100* flowered about 24–25 days later than the wild type with *ca.* 36–37 more leaves under these conditions (Fig. 3*C*). These data are consistent with the known phenotype of *gi* mutants (39). To determine whether the flowering phenotype of *gi-100* was also fully complemented by the wild-type *GI* gene, we examined the flowering time of the transgenically complemented lines under LD conditions. As shown in Fig. 3*C*, these lines flowered early in a manner similar to the wild type, confirming that the insertional disruption at the *gi* locus is primarily responsible for the late flowering phenotype. Additionally, we found that the *gi-100* mutant failed to complement the late flowering phenotypes of *gi-1* and *gi-2* when crossed with

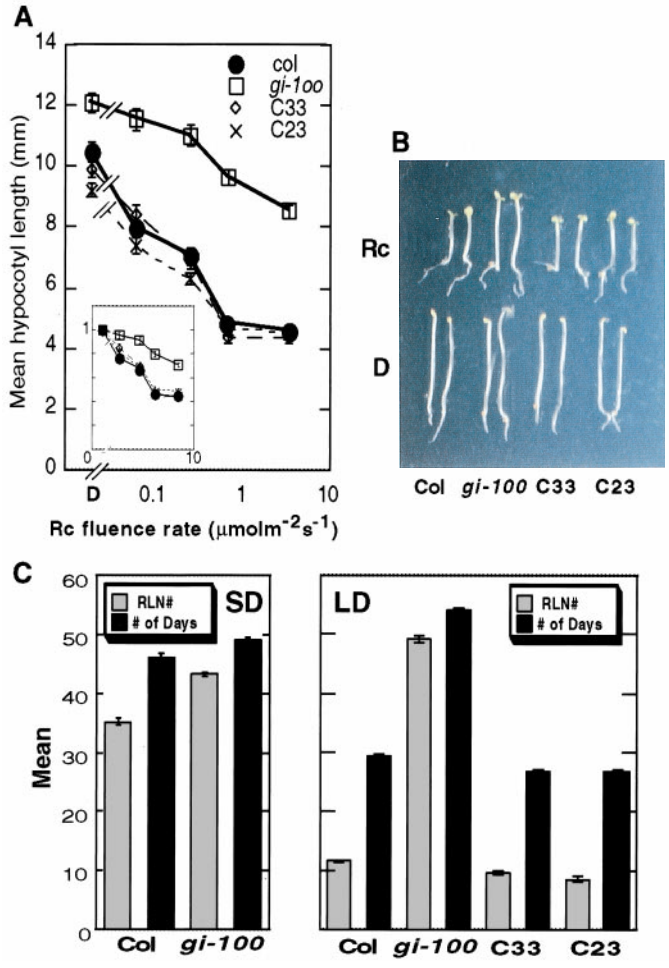

Fig. 3. Complementation of *gi-100* mutant with wild-type *GI* locus. (*A*) Fluence-rate response curves for hypocotyl lengths of two complemented lines (C33 and C23) along with wild-type (Col) and *gi-100* mutant seedlings grown in darkness (D) or a range of Rc fluence rates for 3 days. Hypocotyl length expressed as percentage of dark value is shown in the inset. Data are expressed as mean ± SEM. (*B*) Visual phenotypes of the two complemented lines (C33 and C23), *gi-100*, and wild type grown either in D or in Rc (3.84 μmolm^{-2}s^{-1}). (*C*) Complementation of the *gi-100* late flowering phenotype with the wild-type *GI* locus. Rosette leaf number (RLN#) or days were counted when the plants bolted under SD (*Left*; 9 h white light of 128 μmolm^{-2}s^{-1} and 15 h dark) or LD (*Right*; 18 h white light of 62 μmolm^{-2}s^{-1} and 6 h dark) at 21°C. Flowering time for the wild type (Col), *gi-100* mutant and the two complemented lines (C33 and C23) are shown. Data are expressed as mean ± SEM.

these mutants, confirming genetically that the *gi-100* is allelic to *gi-1* and *gi-2* (data not shown).

GI Is Localized to the Nucleus. Computer analysis of the GI amino acid sequence predicted six transmembrane helices indicative of an integral membrane protein (data not shown, and refs. 23 and 24). This observation has led to the conclusion that GI may be a plasmamembrane protein (23). To investigate the subcellular location of GI, we fused the full-length polypeptide or various fragments thereof to the C terminus of GUS or GFP (Fig. 4*A*). Surprisingly, the GUS-full-length-GI fusion protein (construct II) was clearly targeted to the nucleus in a transient transfection assay, in contrast to the GUS alone control (construct I), which, as expected, was distributed throughout the cell (Fig. 4*B*) (19). The localization visualized in Fig. 4*B* was verified by semiquantitative analysis of the subcellular distribution of GUS. In this analysis, we visually scored each transiently transfected cell and assigned it to one of five classes based on the intensity of GUS staining in the nucleus compared with the cytosol (Fig. 4*C*). This analysis provides quantitative evidence that GUS-GI (construct II) is primarily targeted to the nucleus compared with the GUS alone control (construct I) (Fig. 4*C*). We also tested whether light has any effect on nuclear localization of GI and found that GUS-GI is constitutively located in the nucleus regardless of dark or light treatment (data not shown).

Together with the prediction of an integral membrane location, the nuclear localization of GUS-GI raised the possibility that GI might be localized to the nuclear membrane. To test more directly for the subnuclear location of GI, we made a GFP-GI fusion construct (construct VII; Fig. 4*A*) and examined GFP distribution by optical sectioning with confocal microscopy. GFP fluorescence was found to be localized to the nucleus and homogenously distributed throughout the interior of the nuclear compartment, providing evidence against an exclusive membrane localization of GI (Fig. 4*D*).

In an initial attempt to localize the region of GI that is responsible for nuclear localization, we made four additional GUS-GI constructs containing subdomains of GI (construct III to VI; Fig. 4*A*) and performed semiquantitative analysis of fusion-protein distribution. Construct III encompassing the N-terminal domain of GI with all of the predicted transmembrane helices (Fig. 4*A*) was found to be predominantly in the cytosol (Fig. 4*C*). Similarly, construct IV representing the remaining C-terminal domain lacking predicted transmembrane segments (Fig. 4*A*) also displayed a distinct skewing toward cytosolic localization compared with the full-length GI construct (Fig. 4*C*). Because neither half of the molecule appeared to localize to the nucleus, the data suggested that a critical component of the normal nuclear localization signal might have been disrupted by the partitioning of the molecule. Consistent with this possibility, constructs V and VI (Fig. 4*A*) were both found to be primarily nuclear localized similar to the full-length GI (Fig. 4*C*). These results suggest that the region of GI between residues 543 and 783 is sufficient for its nuclear localization. This region contains four separate clusters of basic amino acids (Fig. 4*E*) similar to clusters established to function as nuclear localization signals (NLSs) in other proteins (33–35).

Discussion

Phytochromes are well documented to pleiotropically control multiple aspects of light-induced plant development throughout the life cycle (1). It may be predicted therefore that genetic screens focused on separate, limited segments of the life cycle may identify the same loci involved in phytochrome signaling. Indeed, such an approach has identified putative early phytochrome signaling-intermediate mutants such as *pef2* and *pef3* by isolating early flowering mutants (8). The coincident identification of *GI* in separate screens for seedling-deetiolation and flowering-time mutants extends these examples.

Our results demonstrate that the *gi-100* mutant is both hyposensitive to Rc at the seedling stage and late flowering as an adult. Two lines of evidence show that both phenotypic traits are because of the insertion at the *GI* locus: (*i*) other mutations in the same gene, *gi-1* and *gi-2*, also have slightly longer hypocotyls under Rc (Fig. 1*A*), and (*ii*) the wild-type *GI* locus complemented both the long hypocotyl and late flowering phenotypes in the *gi-100* mutant (Fig. 3). A previous report that *gi-2* had long hypocotyls under white light (36) is consistent with our data obtained using phytochrome-targeted monochromatic light. The reduced responsiveness of *gi* mutant seedlings to Rc (Fig. 1) indicates that GI is required for the phyB signaling pathway. Conversely, the absence of a substantial alteration in responsiveness to FRc in the mutant suggests that GI does not play a major role in phyA signaling.

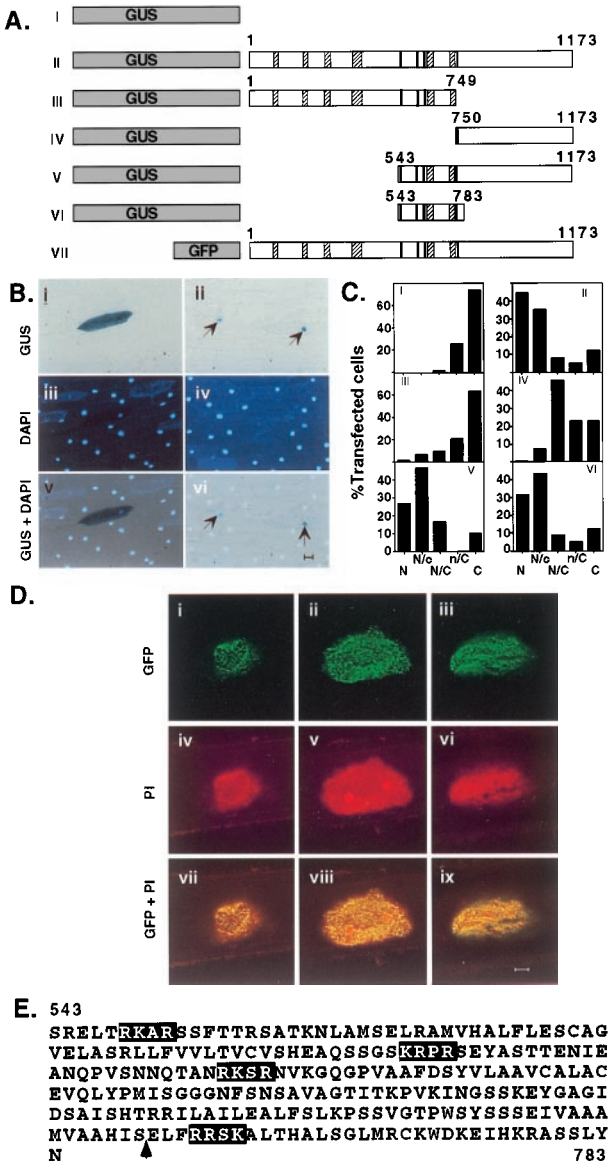

Fig. 4. GI localizes to the nucleus. (*A*) Schematic representations of GUS-GI and GFP-GI fusion constructs used in transient assays. The hatched boxes represent computer-predicted putative membrane spanning domains, and the black bars represent clusters of residues in which three of four are basic amino acids. (*B*) Transient transfection assay in onion epidermal cells using GUS-GI constructs. Top pair of panels show GUS staining for (*i*) GUS only control (construct I) and (*ii*) GUS-GI (construct II). Middle panels (*iii* and *iv*) show 4′,6-diamidino-2-phenylindole (DAPI) staining for nuclei of the cells in the above panels. Bottom panels (*v* and *vi*) show superimposition of the above two panels in each case to show colocalization. Arrows in *ii* and *vi* indicate position of GUS-stained nuclei. (Bar = 100 μM.) (*C*) Bar graphs showing quantitation of the subcellular localization of each GUS-GI construct shown in *A*. Panel numbering corresponds to the construct designated in *A*. Individual onion cells transiently expressing each construct were visually scored for GUS distribution after 3 h incubation and assigned to one of five categories: N, completely nuclear; C, completely cytosolic; N/C, 50% nuclear and 50% cytosolic; N/c, 75% nuclear and 25% cytosolic; n/C, 25% nuclear and 75% cytosolic. (*D*) 2 μm optical sections of top (*i*, *iv*, and *vii*), middle (*ii*, *v*, and *viii*) and bottom (*iii*, *vi*, and *ix*) regions of a nucleus transformed with GFP-GI (construct VII) scanned at 1024 × 1024 pixel resolution with a 25× oil objective. Upper row of panels shows GFP fluorescence (*i*, *ii*, and *iii*), middle row of panels shows propidium iodide (PI) staining of the nuclear DNA (*iv*, *v*, and *vi*), and the bottom row of panels shows merging of the corresponding upper two panels to show colocalization (*vii*, *viii*, and *ix*). (Bar = 10 μM.) (*E*) Amino acid sequence from residue 543 to 783 of GI showing the clusters of basic amino acids (reverse contrast). Arrow indicates the junction between amino acids 749 and 750.

The Rc-selective long-hypocotyl phenotype appears to be more pronounced for the *gi-100* allele than for *gi-1* and *gi-2*. The basis for this difference is not clear. *gi-1* and *gi-2* are capable of expressing about 1,000 and 200 amino acids of the N-terminal region of the protein, respectively (23), whereas *gi-100* is capable of expressing 706 amino acids of the N-terminal region based on the location of the T-DNA insert and Northern blot results (Fig. 2). Therefore, it does not appear that the point at which the potential protein product is truncated can account for the differences in phenotype. On the other hand, the level of the truncated *GI* transcript is somewhat increased in the *gi-100* mutant compared with wild type (Fig. 2), in contrast to the *gi-1* and *gi-2* mutants where *GI* transcript levels are reduced (23). It is possible that the increased hyposensitivity conferred by these three alleles is because of a dominant negative effect exerted by the truncated fragments of GI potentially titrating out a factor required for inhibiting hypocotyl elongation. The difference in severity between these alleles might then be explained by the increased level of expression of the *gi-100* allele compared with the reduced level of expression of the *gi-1* and *gi-2* alleles.

The above data suggest that GI is involved in phyB signaling in seedlings under Rc, and imply that this protein may also function as a phyB signaling intermediate in photoperiodic control of flowering. This proposition is at least superficially consistent with current genetic models for the roles of various flowering-time genes in *Arabidopsis* which suggest that GI is involved in the photoperiodic promotion pathway (37). Moreover, the involvement of GI in phyB-signaling is also consistent with the proposition that GI functions, at least in part, in controlling light signaling to the circadian clock (24). On the other hand, the formal mechanism by which GI might function as a common phyB signaling intermediate in the dual control of these two divergent and temporally separate developmental processes is not immediately clear. The simplest interpretation of our seedling data is that GI acts positively in the phyB signaling pathway controlling deetiolation, because loss of function mutants in either phyB itself (4, 38) or GI (Fig. 1*B*) both result in reduced deetiolation in Rc. By contrast, loss of function mutants in phyB or GI have diametrically opposite effects on floral induction in response to different photoperiods: In SD, *phyB* mutants flower early, whereas *gi* mutants flower at the same time or even later than wild type (ref. 39; Fig. 3*C*). Conversely, in LD *gi* mutants flower late, whereas *phyB* mutants flower at the same time or even earlier than wild type (ref. 39; Fig. 3*C*). This apparent discrepancy between seedling and adult responses might eventually be explained by the differences in the nature of the inductive signals used for each response, and the differences in complexity of the two responses themselves. Alternatively, the molecular function of GI might be developmentally regulated such that its role in phyB signaling in seedling deetiolation is not maintained in the adult, but is instead modified for participation in a different way in floral induction. Given that *GI* expression can be circadianly regulated (23, 24), the long hypocotyl phenotype of *gi* might have been explained by circadian dysfunction, as found for the *elf3* mutant under light/dark cycles (40). However, this appears unlikely because the seedlings in our experiments were grown under Rc from germination without any light/dark cycle entrainment. We conclude, therefore, that GI might use a novel mechanism for controlling both hypocotyl elongation and flowering time.

The consequences of the demonstration that GI appears to constitutively localize to the nucleoplasm are severalfold. First, the data contradict previous computer-based predictions of a plasmamembrane localization (23), thereby redirecting considerations of the possible cellular function of GI. Second, GI joins the growing list of nuclear proteins involved in early phytochrome signaling (13, 18, 19), thus contributing to the emerging notion that early signaling events are nuclear localized. Third,

the evidence that GI is localized to the nucleoplasm rather than the nuclear membrane suggests a possible role in transcriptional regulation. Indeed, the expression patterns of *CAB*, *LHY*, and *CCA1* are altered in *gi* mutants compared with the wild type, indicating that GI may have a role in phytochrome-regulated transcription of circadian controlled genes (23, 24).

Our preliminary effort to map the NLSs of GI has shown that the central ≈241 amino acid region (residues 543 to 783) is sufficient for nuclear targeting (Fig. 4*C*). Moreover, the data show that bisecting the protein between residues 749 and 750 within this region disrupts a critical determinant for nuclear localization. This region contains four clusters of basic amino acids (Fig. 4*E*). Bisection of GI at the 749/750 junction separates the C-terminal-most basic cluster from the three upstream clusters (Fig. 4 *A* and *E*). Because this separation disrupts the capacity for nuclear localization in the two resulting fragments (constructs III and IV; Fig. 4 *A* and *C*), and because, conversely, inclusion of the C-terminal basic cluster together with the other three in the central domain reinstates nuclear localization (construct VI; Fig. 4 *A* and *C*), it appears that the C-terminal cluster may function together with one or more of the other three to facilitate nuclear targeting. These four basic clusters are individually similar to clusters observed in established bipartite NLSs in other nuclear proteins (33–35). However, whereas the distance between pairs of such clusters in these typical bipartite NLSs is 10–12 amino acids, the separation in GI is 56, 23, and 114 amino acids. It is possible, therefore, that the C-terminal basic cluster might be topologically located near one of the upstream clusters in the folded GI protein in a manner similar to bipartite NLSs, despite the long intervening stretch of polypeptide, and might thereby function as an atypical bipartite NLS. Alternatively, the presence of all four basic clusters might be necessary to provide efficient nuclear localization as has been observed in some other proteins containing multiple NLSs (35).

Taken together, the data presented here suggest a complex and potentially novel role of GI in phyB-signal transduction at distinctly different phases of the life cycle. Elucidation of the molecular basis for this signaling function will provide valuable insight into the mechanisms by which the phytochromes exert pleiotropic control of plant developmental responses to the light environment.

We thank Y. Kang for excellent technical assistance, C. Fairchild and M. Hudson for critical reading of the manuscript, D. Schichnes for assistance with the confocal microscope, D. Somers for providing *gi-1* and *gi-2* seeds, and the *Arabidopsis* Biological Resource Center for providing seed stocks and *Arabidopsis* cDNA library. This work was supported by grants from the Department of Energy Basic Energy Sciences number DE-FG03–87ER13642 and U.S. Department of Agriculture Current Research Information Service number 5325-21000-010-00D.

1. Kendrick, R. E. & Kronenberg, G. H. M. (1994) *Photomorphogenesis in Plants* (Kluwer, Dordrecht, The Netherlands), 2nd Ed.
2. Sharrock, R. A. & Quail, P. H. (1989) *Genes Dev.* **3,** 1745–1757.
3. Clack, T., Mathews, S. & Sharrock, R. A. (1994) *Plant Mol. Biol.* **25,** 413–426.
4. Quail, P. H., Boylan, M. T., Parks, B. M., Short, T. W., Xu, Y. & Wagner, D. (1995) *Science* **268,** 675–680.
5. Ni, M., Tepperman, J. M. & Quail, P. H. (1999) *Nature (London)* **390,** 781–784.
6. Deng, X.-W. & Quail, P. H. (1999) *Semin. Cell Dev. Biol.* **10,** 121–128.
7. Martinez-Garcia, J. F., Huq, E. & Quail, P. H. (2000) *Science* **288,** 859–863.
8. Ahmad, M. & Cashmore, A. R. (1996) *Plant J.* **10,** 1103–1110.
9. Wagner, D., Hoecker, U. & Quail, P. H. (1997) *Plant Cell* **9,** 730–743.
10. Halliday, K. J., Hudson, M., Ni, M., Qin, M.-M. & Quail, P. H. (1999) *Proc. Natl. Acad. Sci. USA* **96,** 5831–5837.
11. Huq, E., Kang, Y., Halliday, K. J., Qin, M.-M. & Quail, P. H. (2000) *Plant J.*, in press.
12. Whitelam, G. C., Johnson, E., Peng, J., Carol, P., Anderson, M. L., Cowl, J. S. & Harberd, N. P. (1993) *Plant Cell* **5,** 757–768.
13. Hudson, M., Ringli, C., Boylan, M. T. & Quail, P. H. (1999) *Genes Dev.* **13,** 2017–2026.
14. Soh, M. S., Hong, S. H., Hanzawa, H., Furuya, M. & Nam, H. G. (1998) *Plant J.* **16,** 411–419.
15. Hoecker, U., Xu, Y. & Quail, P. H. (1998) *Plant Cell* **10,** 19–32.
16. Genoud, T., Millar, A. J., Nishizawa, N., Kay, S. A., Schäfer, E., Nagatani, A. & Chua, N. H. (1998) *Plant Cell* **10,** 889–904.
17. Neff, M. M., Fankhauser, C. & Chory, J. (2000) *Genes Dev.* **14,** 257–261.
18. Hoecker, U., Tepperman, J. M. & Quail, P. H. (1999) *Science* **274,** 496–499.
19. Ni, M., Tepperman, J. M. & Quail, P. H. (1998) *Cell* **95,** 657–667.
20. Sakamoto, K. & Nagatani, A. (1996) *Plant J.* **10,** 859–868.
21. Kircher, S., Kozma-Bognar, L., Kim, L., Adam, E., Harter, K., Schäfer, E. & Nagy, F. (1999) *Plant Cell* **11,** 1445–1456.
22. Nagy, F. & Schäfer, E. (2000) *EMBO J.* **19,** 157–163.
23. Fowler, S., Lee, K., Onouchi, H., Samach, A., Richardson, K., Morris, B., Coupland, G. & Putterill, J. (1999) *EMBO J.* **18,** 4679–4688.
24. Park, D. H., Somers, D. E., Kim, Y. S., Choy, Y. H., Lim, H. K., Soh, M. S., Kim, H. J., Kay, S. A. & Nam, H. G. (1999) *Science* **275,** 1579–1582.
25. Wagner, D., Tepperman, J. M. & Quail, P. H. (1991) *Plant Cell* **3,** 1265–1278.
26. Weigel, D., Ahn, J. H., Blazquez, M. A., Borevitz, J. O., Christensen, S. K., Fankhauser, C., Ferrandiz, C., Kardailsky, I., Malancharuvil, E. J., Neff, M. M., *et al.* (2000) *Plant Physiol.* **122,** 1003–1013.
27. Kieber, J. J., Rothenberg, M., Roman, G., Feldmann, K. A. & Ecker, J. R. (1993) *Cell* **72,** 426–441.
28. Church, G. M. & Gilbert, W. (1984) *Proc. Natl. Acad. Sci. USA* **81,** 1991–1995.
29. Hajdukiewicz, P., Svab, Z. & Maliga, P. (1994) *Plant Mol. Biol.* **25,** 989–994.
30. Clough, S. J. & Bent, A. F. (1998) *Plant J.* **16,** 734–743.
31. Restrepo, M. A., Freed, D. D. & Carrington, J. C. (1990) *Plant Cell* **2,** 987–998.
32. von Arnim, A. G., Deng, X.-W. & Stacey, M. G. (1998) *Gene* **221,** 34–43.
33. Dehesh, K., Smithe, L. G., Tepperman, J. M. & Quail, P. H. (1995) *Plant J.* **8,** 25–35.
34. Hicks, G. R. & Raikhel, N. V. (1995) *Annu. Rev. Cell Dev. Biol.* **11,** 155–188.
35. Jans, D. A. & Hübner, S. (1996) *Physiol. Rev.* **76,** 651–685.
36. Araki, T. & Komeda, Y. (1993) *Plant J.* **3,** 230–238.
37. Levy, Y. Y. & Dean, C. (1998) *Plant Cell* **10,** 1973–1989.
38. Reed, J. W., Nagpal, P., Poole, D. S., Furuya, M. & Chory, J. (1993) *Plant Cell* **5,** 147–157.
39. Koornneef, M., Hanhart, C., van Leonen-Martinet, P. & de Vries, H. B. (1995) *Physiol. Plant.* **95,** 260–266.
40. Dowson-Day, M. J. & Millar, A. J. (1999) *Plant J.* **17,** 63–71.